

Half-Rounded Circular Overflow - On Cavity Transients and Non Linear Instabilities

Hubert Chanson⁽¹⁾

⁽¹⁾ The University of Queensland, School of Civil Engineering, Brisbane QLD 4072, Australia
E-mail: h.chanson@uq.edu.au

Abstract

Liquid overflowing over rounded weirs experiences a rapidly accelerating fluid flow region near the crest. Depending upon the discharge and radius of curvature, the overflow nappe may be attached or detached. Herein, careful physical modelling was conducted under carefully controlled conditions with a circular weir equipped with a relatively small radius of curvature. Based upon simple experiments across a very broad range of flow rates, the results highlighted a narrow range of hydrodynamic transient conditions for which both attached and detached nappe situations may co-exist. Cavity transients were observed as a result of non-linear instabilities at both detachment and re-attachment. The transients were characterised by massive non-linear instabilities, associated with very rapid change in hydrodynamic properties, and sometimes loud acoustics and impact on the weir structure. The hydrodynamic processes presented some form of hysteresis.

Keywords: Circular crested weirs, Fluid-structure interactions, Hydrodynamic instabilities, Physical modelling, Air cavity transients

1. INTRODUCTION

Weirs are hydraulic structures typically built across a river to facilitate the storage of water and raise the upstream water level (USBR 1965). Smaller weirs are also used in industrial facilities. Liquid flowing over rounded weirs experiences a rapidly accelerating fluid flow region near the crest, characterised by strong streamline curvature (Fawer 1937, Sarginson 1972, Ramamurthy and Vo 1993). The discharge characteristic curve of the structure is a function of the weir geometry, roughness, and inflow conditions (Chanson and Montes 1998). For small to medium upstream heads, the circular weir overflow is more stable than sharp-crested weir overflows, has a greater discharge capacity than broad-crested weir, and the design and construction is simpler than the ogee crest design. Thus, the circular-crest shape remains commonly utilised into the 21st century, e.g. for lateral spillways (Fig. 1). Figure 1 presents the half-round circular crest along the lateral spillway of Sorpe Dam (Germany).

Recently, a test case study of round-crested weirs reported a number of discrepancies among 20 data sets obtained at 20 different hydraulic facilities across our planet for the same boundary condition specifications: "*the experimental results found significant variability in the discharge coefficients as a function of dimensionless upstream head, as well as in the head-discharge relationships (as much as 50% in some cases)*" (Tullis et al. 2019). A subsequent study with half-round circular crested weir pointed out to the existence of hydrodynamic hysteresis and flow instabilities: "*the data showed some hysteresis, with different results depending on whether the experiments were conducted with increasing or decreasing discharges*"; "*long-duration cyclic behaviors were recorded [...] including large transverse instabilities of the lower nappe impingement into the body of water*" (Chanson 2020). Both studies acknowledged several "types of [error] sources" (Tullis et al. 2019, p. 498) and stressed the "*the importance of the quality of experimental setup and expertise of the individual experimentalist*" (Chanson 2020, p. 04020008-5).

This contribution aims to discuss the transient processes during nappe detachment and re-attachment and the associated hydrodynamic instabilities on a half-rounded circular weir (Fig. 2). The investigations were undertaken under carefully-controlled flow conditions. The results contain some physical characterisation of air cavity collapse and appearance processes. The work aims to gain new information for the estimation of unsteady hydrodynamic loads on circular crested weirs.



Figure 1. Half-round circular-crested weir at Sorpe Dam (Germany) on 31 March 2004.



Figure 2. Overflow experiments on half-round circular weir with flow direction from right to left. Left: detached nappe for $q = 0.0426 \text{ m}^2/\text{s}$, $(H-P)/r = 7.19$; Right: attached nappe for $q = 0.0554 \text{ m}^2/\text{s}$, $(H-P)/r = 7.94$.

2. PHYSICAL STUDY AND INSTRUMENTATION

The experiments were performed in the Hydraulics Laboratory of the Advanced Engineering Building (AEB) at the University of Queensland (UQ). The study was conducted in a 3.0 m long 0.4 m wide horizontal channel. The bed and sidewalls were in PVC and glass respectively (Fig. 2). Upstream, the water was delivered through a three-dimensional convergent connected to a deep and wide intake basin, fed by a constant head tank and water reticulation system. The arrangement provided a constant discharge with smooth inflow conditions to the flume's upstream end. At the downstream end, the channel ended with a free overfall.

The half-round circular crested weir was placed 1.34 m downstream of the test section's start, at right angle across the channel bed (Fig. 2), at the same location as Chanson (2020). The weir design followed Tullis et al. (2019). It was 0.020 m thick and the crest height was $P = 0.250 \text{ m}$ above the channel bed. The

half-round crest had a radius $r = 0.010$ m. Both the crest and weir were machined out of PVC with an accuracy of 0.2 mm. As shown in Figure 2, the nappe was not ventilated.

The water discharge was measured with a 90° V-both weir, extensively calibrated in-house (Chanson and Wang 2013). The water surface elevations were recorded with pointer gauges. Visual, photographic and cinematographic data were collected using dSLR cameras Pentax™ with sensor resolutions between 24 Mpx and 26 Mpx, complemented by a digital camera Sony™ RC100VA, and an iPhone XI. The dSLR cameras were equipped with full-frame prime lenses producing both photographs and movies with negligible barrel distortion. Movies were recorded with the camera Sony™ RC100VA at 25 fps and 100 fps in 4K and HD resolutions respectively. The typical recording time was 1,800 s (30 minutes) following an earlier recommendation (Chanson 2020), although longer experiments were also conducted. A number of movies were processed using Matlab scripts, as well as the softwares Tracker v. 4.91 and TEMA 2D Motion v. 3.9.

3. BASIC RESULTS

Although the weir was un-ventilated, three type of nappe flow patterns were observed with increasing flow rates. At low discharges, the nappe attached to the crest and to the downstream weir wall. For a range of intermediate flows, the nappe detached (Fig. 2 Left). For large flows, the nappe re-attached to the weir (Fig. 2 Right). As discussed by Chanson (2020), some experimental hysteresis was seen, with some different flow conditions for the changes in nappe flow regime between experiments conducted with either increasing or decreasing discharges.

The dimensionless discharge coefficient data are presented in Figure 3. In Figure 3, the thick solid vertical lines correspond to the "mean" conditions for the change in nappe flow regime. Herein, the dimensionless discharge coefficient is defined based upon a modified form of the Bernoulli principle linking the relationship between unit discharge q and upstream head above crest (H-P):

$$q = C_D \times \sqrt{g \times \left(\frac{2}{3} \times (H - P) \right)^3} \quad [1]$$

The discharge coefficient C_D is typically larger than unity for a circular crested weir, as observed in the current study (Fig. 3) and in previous data sets (Sarginson 1972, Vo 1992, Chanson and Montes 1998). The discharge coefficient data showed some significant scatter, consistent with the data sets reported by Tullis et al. (2019) and Chanson (2020) (Fig. 3). It is thought that some scatter was directly caused by non-linear instabilities observed during long-duration experiments, including the present one. Further, the data set showed a clear hysteresis, with marked differences between data sets recorded with increasing discharges and those with decreasing discharges.

The change in nappe flow regime, from attached to detached, and from detached to attached nappe, induced transient conditions and had some major impact onto the experimental flow patterns. An attached nappe was characterised by a stronger streamline curvature, associated with an increased discharge coefficient, as predicted by irrotational flow theory of ideal fluid (Vallentine 1969, Dressler 1978, Chanson 2014). Thus, the change from detached nappe to attached was linked to a sudden decrease in upstream water level, with the upstream propagation of a negative wave in the upstream reservoir and potentially some reservoir sloshing. At the same time, the transient increase in flow rate over the weir generated a positive surge propagating downstream. The transient change in nappe flow regime further generated unsteady structural loads on the weir wall. Conversely, the change from attached nappe to detached caused the upstream propagation of a positive surge in the reservoir and the downstream propagation of a negative surge in the tailrace channel.

While the current experimental observations showed some hysteresis in the transitions between regimes between experiments with increasing and decreasing discharges, a key experimental observation was the occurrence of two ranges of flow conditions during which a cyclic behaviour was observed. That is, with the formation of a large air cavity, often with some loud noise, followed by the progressing filling of the cavity, then the air cavity disappearance, and again a sudden cavity reopening into a large air cavity while keeping a constant flow rate, as during the current study. The periods of the cyclic pattern were typically between 3 and 10 min, although some unusually wider range of periods, from 1 to 12 min, was observed. These "cyclic" flow conditions were typically observed for dimensionless discharges about $d_c/P \sim 0.21-0.22$ and $d_c/P \sim 0.25-0.31$, with d_c the critical depth $d_c = (q^2/g)^{1/3}$, P the weir height, q the unit discharge and g the gravity acceleration.

Note that, at the crest of the circular weir, the observed water depth d_{crest} differed from d_c because of the non-hydrostatic pressure distribution and non-uniform velocity field (Fawer 1937, Vo 1992, Chanson 2006,2008). It must be stressed that the expression $(q^2/g)^{1/3}$ is the critical depth only for hydrostatic pressures and uniform velocity distribution in a horizontal channel (Bakhmeteff 1932, Chanson 2004).

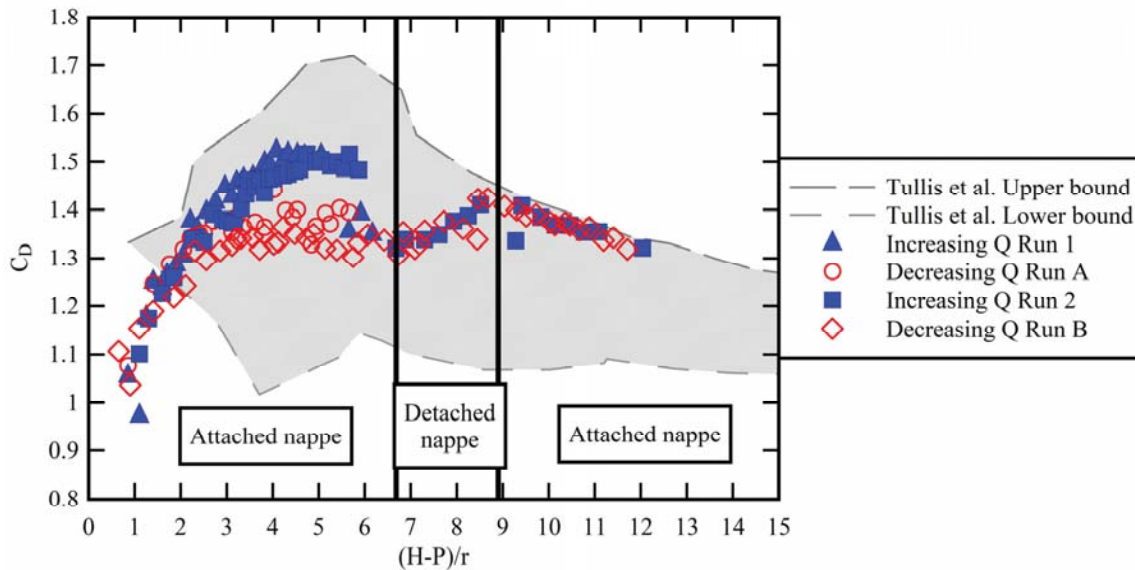


Figure 3. Dimensionless discharge coefficient C_D for the half-round circular-crested weir. Comparison with the data range of Tullis et al. (2019).

4. HYDRODYNAMIC INSTABILITIES AND NON-LINEARITIES

During the physical experiments, the cyclic behaviour in changes in nappe flow patterns took place over a relatively broad range of flow rates. Long duration experiments were conducted for flow conditions close to these transitional conditions. First, the flow conditions were established for 30 minutes minimum before any observations. Then, the measurements were undertaken for a further 30 minutes and often repeated over several hours. During that time, the flow rate was checked regularly, e.g. every ten minutes, and remained unchanged. Figure 4 illustrates a typical cyclic pattern between nappe detachment and re-attachment, recorded for 30 minutes. In Figure 4, the dimensionless air cavity volume is presented as a function of time. A zero cavity volume would correspond to a complete air cavity collapse and a re-attached nappe, as illustrated in Figure 3 (Right).

The data indicated fast fluctuations super-imposed on slow fluctuations. This is illustrated in Figure 4, with the instantaneous time series in thin line and the smoothed trendline in thick line. For this data set - Figure 4 , 17 cavity collapses and nappe re-attachments were seen for the 30-minutes long record. Overall, the instantaneous data demonstrated that the cavity opening was a very rapid transient feature, with a very rapid initial cavity expansion, lasting less than one second. This initial stage was often violent and accompanied by a loud low-frequency noise which could be heard from quite far away - e.g. in the entire floor of the building. This initial transient was followed by a period of slower cavity expansion, which could span up to a dozen of seconds. By contrast, the air cavity filling was always a relatively slow process, lasting several minutes.

During the transitional flow conditions, a cyclic behaviour was observed not only in terms of the air cavity characteristics (height, length, volume) but also in terms of the water depth d_{crest} at the weir crest and upstream water depth d_1 . Depending upon the flow rate, the cyclic behaviour could correspond to cyclic patterns between a detached nappe and an attached nappe - as seen in Figure 4, cyclic patterns between a detached nappe and a partially-attached nappe with a very small air cavity, or a mix between these two cyclic patterns. Figure 5 summarises observations on the mean period of nappe instability (attachment/detachment) and percentage of total air cavity collapse events during a 30 minutes record for $0.25 < d/P < 0.31$. Figure 5 shows the change in cyclic behaviour of nappe detachment/re-attachment across a relatively narrow range of flow conditions.

The physical processes associated with the cyclic nappe overflow pattern may induce vibrations to the weir wall and even impact on the structural stability of thin-walled weirs, during high-intensity transients. Furthermore, the hydrodynamic instabilities may interact with oscillations of the air volume trapped beneath the nappe, leading to adverse resonance effects (Rockwell and Naudasher 1978, Petrikat 1978). Most notable features of these interactions include the horizontal banding on the nappe, the low frequency acoustic energy resulting in low rumble noise that can be heard, and un-necessary vibrations to the weir itself.

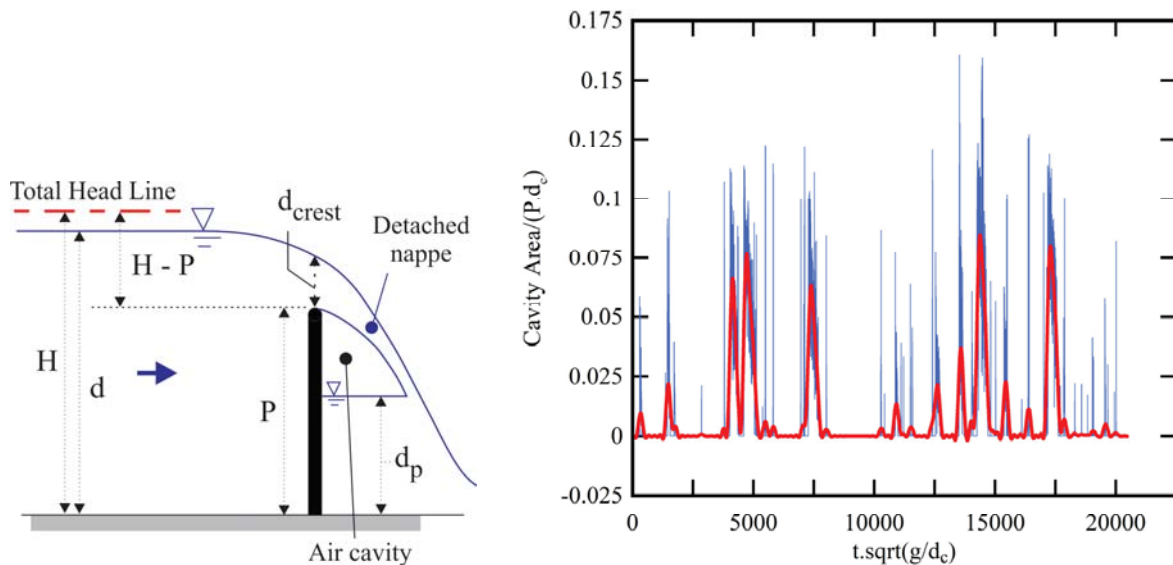


Figure 4. Dimensionless time variation of air cavity volume during half-round circular-crested weir overflow for $q = 0.06425 \text{ m}^2/\text{s}$, $(H-P)/r = 9.4$. Inset (Left): definition sketch.

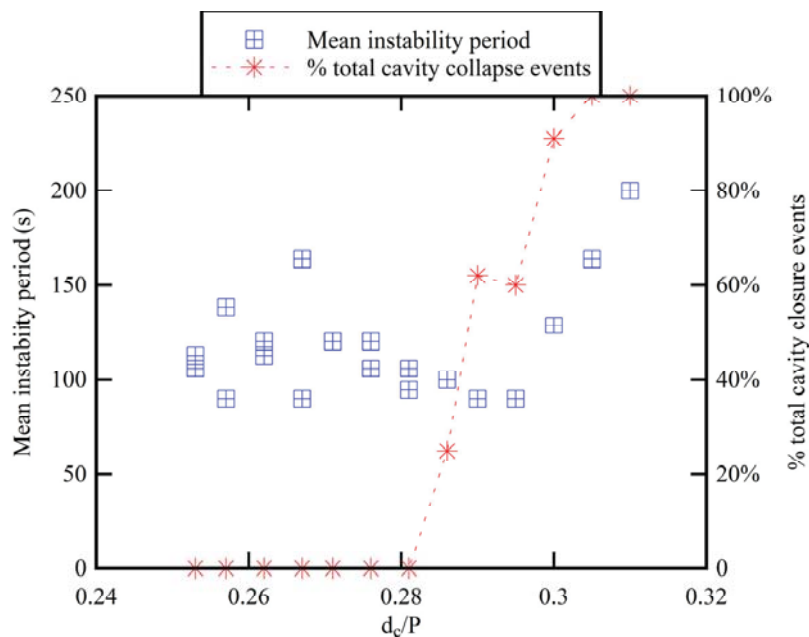


Figure 5. Dimensionless time variation of mean period of nappe instability (attachment/detachment) and percentage of total air cavity collapse events during a 30 minutes record.

5. CONCLUSION

New experiments were conducted on an un-ventilated half-round circular-crested weir across a relatively large range of flow conditions. A key feature of the flow pattern was whether the overflow nappe was attached or detached. The observations of nappe flow patterns presented some hysteresis with different quantitative results recorded depending on whether the experiments were conducted with increasing or decreasing flow

rates. Despite a very careful experimental protocol, the current results in terms of dimensionless discharge coefficient showed some large data scatter, consistent with prior relevant studies (Tullis et al. 2019, Chanson 2020). It is thought that the scatter was directly caused by the existence of non-linear instabilities.

For the flow conditions close to the transition between nappe flow patterns, some cyclic patterns between attached and detached nappe developed while the flow rate remained constant, and it is believed that the cyclic behaviour of the weir was linked to the absence of nappe ventilation. Long-duration experiments were used to document carefully the cyclic behaviour under constant controlled flow rate. The results showed that large instabilities occurring at very low frequencies. Practically, the findings implied that physical modelling only conducted over short periods might not be extrapolated to full-scale without adverse scaling impacts for these transitional conditions. More, both qualitative and quantitative observations showed that the air cavity filling was a slow process lasting several minutes, when the cavity formation was a very rapid transient, sometimes violent with loud noise. The latter, i.e. cavity detachment, would required high frequency sampling to be properly documented. Altogether, the present study illustrated some complicated hydrodynamic patterns for which the quality of the experimental setup and expertise of the individual experimentalists are critical parameters to document accurately and precisely the flow instabilities. Implicitly, the present work highlights some major limitations of physical and numerical modelling, including CFD modelling with commercial software on desktop workstations - which would not detect these transient hydrodynamic processes.

6. ACKNOWLEDGEMENTS

The author acknowledges the technical assistance of Jason Van Der Gevel, Stewart Matthews and Dr Youkai Li (The University of Queensland) and his student Oscar Memory for data collection. The financial support of the School of Civil Engineering at the University of Queensland (Australia) is acknowledged.

7. REFERENCES

- Bakhmeteff, B.A. (1932). "Hydraulics of Open Channels." *McGraw-Hill*, New York, USA, 1st ed., 329 pages.
- Chanson, H. (2004). "The Hydraulics of Open Channel Flow: An Introduction." *Butterworth-Heinemann*, 2nd edition, Oxford, UK, 630 pages.
- Chanson, H. (2006). "Minimum Specific Energy and Critical Flow Conditions in Open Channels." *Journal of Irrigation and Drainage Engineering*, ASCE, Vol. 132, No. 5, pp. 498-502 (doi:10.1061/(ASCE)0733-9437(2006)132:5(498)).
- Chanson, H. (2008). "Minimum Specific Energy and Critical Flow Conditions in Open Channels - Closure." *Journal of Irrigation and Drainage Engineering*, ASCE, Vol. 134, No. 6, pp. 883-887 (DOI: 10.1061/(ASCE)0733-9437(2008)134:6(883))
- Chanson, H. (2014). "Applied Hydrodynamics: An Introduction." *CRC Press*, Taylor & Francis Group, Leiden, The Netherlands, 448 pages & 21 video movies (ISBN 978-1-138-00093-3).
- Chanson, H. (2020). "Half-round Circular Crested Weir: On Hysteresis, Instabilities and Head-Discharge Relationship." *Journal of Irrigation and Drainage Engineering*, ASCE, Vol. 146, No. 6, Paper 04020008, 7 pages & 3 video movies (DOI: 10.1061/(ASCE)IR.1943-4774.0001473).
- Chanson, H., and Montes, J.S. (1998). "Overflow Characteristics of Circular Weirs: Effect of Inflow Conditions." *Journal of Irrigation and Drainage Engineering*, ASCE, Vol. 124, No. 3, pp. 152-162 (DOI: 10.1061/(ASCE)0733-9437(1998)124:3(152)).
- Chanson, H., and Wang, H. (2013). "Unsteady Discharge Calibration of a Large V-notch Weir." *Flow Measurement and Instrumentation*, Vol. 29, pp. 19-24 & 2 videos (DOI: 10.1016/j.flowmeasinst.2012.10.010).
- Dressler, R.F. (1978). "New Nonlinear Shallow-Flow Equations with Curvature." *Journal of Hydraulic Research*, IAHR, Vol. 16, No. 3, pp. 205-222.
- Fawer, C. (1937). "Etude de Quelques Ecoulements Permanents à Filets Courbes." *Thesis*, Lausanne, Switzerland, Imprimerie La Concorde, 127 pages (in French).
- Petrikat, K. (1978). "Model Tests on Weirs, Bottom Outlet Gates, Lock Gates and Harbours Moles." *M.A.N. Technical Bulletin*, Nurnberg, Germany, 36 pages.
- Ramamurthy, A.S., and Vo, N.D. (1993). "Application of Dressler Theory to Weir Flow." *Journal of Applied Mechanics*, Trans. ASME, Vol. 60, No. 1, pp. 163-166.
- Rockwell, D., and Naudascher, E. (1978). "Self-sustained oscillations of impinging free shear layers." *Annual Review of Fluid Mechanics*, Vol. 11, pp. 67-94.
- Sarginson, E.J. (1972). "The Influence of Surface Tension on Weir Flow." *Journal of Hydraulic Research*, IAHR, Vol. 10, No. 4, pp. 431-446.

- Tullis, B.P., Crookston, B.M., and Bung, D.B. (2019). "Weir head-discharge relationships: A multilab exercise." *Proc. 38th IAHR World Congress*, Panama City, 1-6 Sept., IAHR Publication, Lucas Calvo Editor, pp. 486-500 (DOI: 10.3850/38WC092019-0806).
- USBR (1965). "Design of Small Dams." *US Department of the Interior*, Bureau of Reclamation, Denver CO, USA, 1st edition, 3rd printing.
- Vallentine, H.R. (1969). "Applied Hydrodynamics." *Butterworths*, London, UK, SI edition.
- Vo, N.D. (1992). "Characteristics of Curvilinear Flow Past Circular-Crested Weirs." *Ph.D. thesis*, Concordia Univ., Canada.